Sensitivity of wind wave simulation to coupling with a tide/surge model with application to the Southern North Sea

J. Monbaliu*, C.S. Yu† and P. Osuna*

Abstract

The wave-current interaction process in a one way coupled system for the Southern North Sea region was studied. To this end, a modified version of the third-generation spectral wave model WAM was run in a three level nested grid system, taking into account the hydrodynamic fields (coupled version) computed by a tide/surge model. The resolution in these three grids corresponds roughly to 35 km (coarse), 5 km (local) and 1 km (fine). Hydrodynamic information was only available at the resolution of the local grid. Results are compared with those of the same version without considering the interaction with tide and surges (uncoupled version). The emphasis is on the results from the local grid calculations. The sensitivity to the source of boundary conditions (coupled vs. uncoupled) and to the frequency of information exchange is investigated. Also the spectral evolution is studied.

Numerical results in the local grid are in good agreement with buoy data. The phase and amplitude of the modulations of wave period observed from the buoy data are quite well reproduced by the coupled version. The model results in the local grid did not show much sensitivity to the source of boundary condition information, nor were they very sensitive to the information update frequency of the hydrodynamic fields. The directional spectra computed in the coupled mode show a broader energy distribution and a more rapid growth. The fine grid results only differ marginally from the local grid results due to the limited resolution of the hydrodynamic fields used.

*Laboratory of Hydraulics, K.U.Leuven, de Croylaan 2, B-3001 Heverlee, Belgium.
†Dept. of Marine Env. and Eng., NSYSU, Lien-Hai Road 70, Kaoshiung 804, Taiwan.

2 The numerical models

2.1 The wave model

The wave model used is the third generation WAM *Cycle_4* model (Günther et al., 1994). The model solves an energy balance equation for the spectrum $\mathrm{F}(f,\theta)$ as a function of the wave frequency, f, wave direction, θ, and the geographical position, x, and time, t. The standard version of WAM propagates the energy over a calculational grid in Cartesian coordinates $\mathrm{x}(x,y)$ for small area applications or in spherical coordinates $\mathrm{x}(\phi,\lambda,r)$ for model applications over large areas as to take into account the swell propagation over great circles. For this work the last option is used. The WAM model permits the inclusion of a stationary current background and uses the relative frequency, σ, as a coordinate. Under these conditions, the energy transport equations solved in the WAM *Cycle_4* model code is equivalent to the action density transport equation. The transport equation for the evolution of the wave spectrum $F(t,\phi,\lambda,\sigma,\theta)$ then reads

$$\frac{\partial F}{\partial t}+(\cos\phi)^{-1}\frac{\partial}{\partial\phi}(\dot{\phi}\cos\phi F)+\frac{\partial}{\partial\lambda}(\dot{\lambda}F)+\sigma\frac{\partial}{\partial\sigma}\left(\dot{\sigma}\frac{F}{\sigma}\right)+\frac{\partial}{\partial\theta}(\dot{\theta}F)=S_{tot}, \qquad (1)$$

where the expressions $\dot{\phi}$, $\dot{\lambda}$, $\dot{\sigma}$, and $\dot{\theta}$ represent the rate of change of energy in the space $(\phi,\lambda,\sigma,\theta)$. At the right hand side of (1), S_{tot} is the function representing the source and sink functions, and the conservative non-linear transfer of energy between wave components. In the present application, it includes wind input S_{in}, non-linear quadruplet wave-wave interactions S_{nl}, whitecapping dissipation S_{ds} and bottom friction dissipation S_{bf}. Standard values were used for the empirical coefficients in the source terms. The model has been used in a quasi–steady approach, assuming that the current and the water depth vary only slowly. A detailed description of the physics incorporated in WAM *Cycle_4* model and its numerical implementation can be found in Komen et al., (1994). Details on the improvements, alterations and additions for application in nearshore regions can be found in Luo and Sclavo (1997) and Monbaliu et al. (1998).

2.2 The tide/surge model

The hydrodynamic (u,v,η) fields are computed with a model based on the shallow water equations. The spherical coordinate expressions for this set of equation are (Washington and Parkinson, 1986)

$$\begin{aligned}\frac{\partial u}{\partial t} &+ \frac{u}{R\cos\phi}\frac{\partial u}{\partial\lambda}+\frac{v}{R}\frac{\partial u}{\partial\phi}-\frac{uv\tan\phi}{R}-2\varpi\sin\phi v\\ &= -\frac{g}{R\cos\phi}\frac{\partial\eta}{\partial\lambda}-\frac{1}{\rho R\cos\phi}\frac{\partial P_a}{\partial\lambda}-\frac{\tau_{b\lambda}}{\rho(h+\eta)}+\frac{\tau_{s\lambda}}{\rho(h+\eta)}\\ &+ A_h\left[\nabla^2 u+\frac{u}{R^2}(1-\tan^2\phi)-2\frac{\tan\phi}{\cos\phi}\frac{\partial v}{\partial\lambda}\right], \qquad (2)\end{aligned}$$

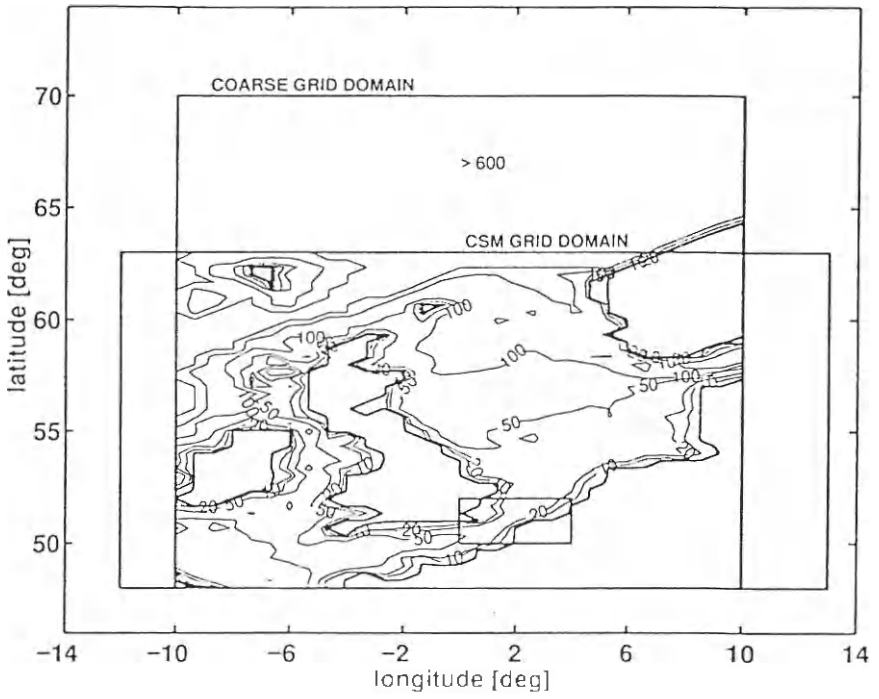

Figure 1: Coarse and CSM grid domain. The coarse grid bathymetry is included. Boundary condition for a nested local grid (region indicated by the square) are generated. Depth values are in meters.

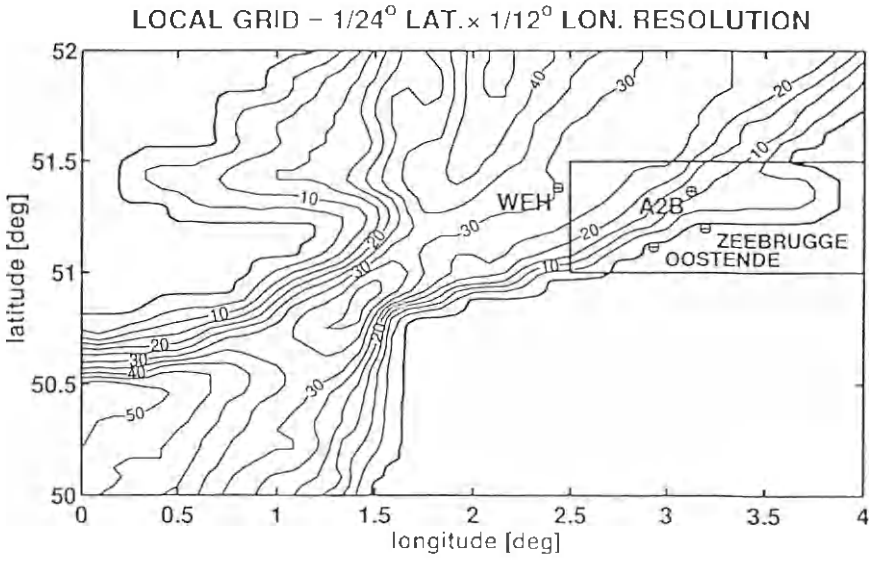

Figure 2: Local grid bathymetry with location indication of the WEH and A2B buoys. Boundary condition for a fine grid (region indicated by the square) are generated. Depth values are in meters.

In what follows, time series at the locations WEH (Westhinder) and A2B from both coupled and uncoupled WAM results are compared with the available buoy data. The sensitivity to 'coupled' information in the boundary conditions, and to the frequency of information exchange is addressed for the local grid application. The evolution of 1D–spectra and 2D–spectra in 'coupled' and 'uncoupled' mode are discussed.

4.2 Time series

Time series calculated by WAM at station WEH (30m depth) show a good agreement with buoy data, especially for significant wave height (Hs) values during high-wave events (see Figure 3). The small modulations visible in the buoy data at WEH seem well reproduced by the coupled version of WAM. However, the presence of some modulations in the uncoupled run results suggests that part of the modulations in the signal must come from wind variability. The bias for Hs in the coupled and uncoupled results is -0.072m and -0.143m, respectively. The intercomparison between results from coupled and uncoupled models show differences (coupled - uncoupled) in Hs smaller than 0.25m, with a mean difference of 0.02m. Modulations of Tm_{02} , corresponding to the dominant semidiurnal tide period, are quite clear in the buoy data (Figure 3). The importance of including the hydrodynamic fields is highlighted qualitatively by the good agreement between buoy data and WAM-coupled results for Tm_{02}. This is not directly reflected in the value for the bias for Tm_{02}, which were 0.032s for the coupled and 0.034s for the uncoupled run, respectively. The model results themselves showed differences up to 1.0s, with a mean difference of -0.15s.

In the more shallow A2B station (11m depth), overestimation of model results with respect to buoy data is observed, both in Hs and in Tm_{02} (Figure 4). Although it is possible to reduce the observed differences by tuning of the empirical coefficient in the bottom friction term (see Luo and Monbaliu, 1994, Luo et al., 1996), this was not done since it was not considered important for the scope of this work. At this station, the bias was -0.128m and -0.116m for Hs and -0.846s and -0.965s for Tm_{02} in the coupled and uncoupled mode, respectively. The importance of tidal modulations is again observed at this location and it is qualitatively well reproduced in the coupled run. Differences between coupled and uncoupled model results do not exceed 0.25m in Hs and 1.0s in Tm_{02}, whereas the mean difference in the Hs and Tm_{02} value was 0.014m and -0.217s, respectively.

4.3 Sensitivity to boundary conditions

In order to explore the necessity to run in coupled mode on a coarse grid in order to supply good boundary conditions for a subsequent nested run, the application on the local grid was run once using boundary conditions from the coupled and once from the uncoupled coarse grid run. In both cases, results showed clearly the tidal modulation effect on Tm_{02} (Figure 5a). The observed differences are small and most of the time do not exceed 5%, which seem to suggest that running the coarse grid

application in coupled mode, does not have a dramatic influence on the local grid runs. Tide–induced modulations, at least on the space scales used here, are mainly a local effect.

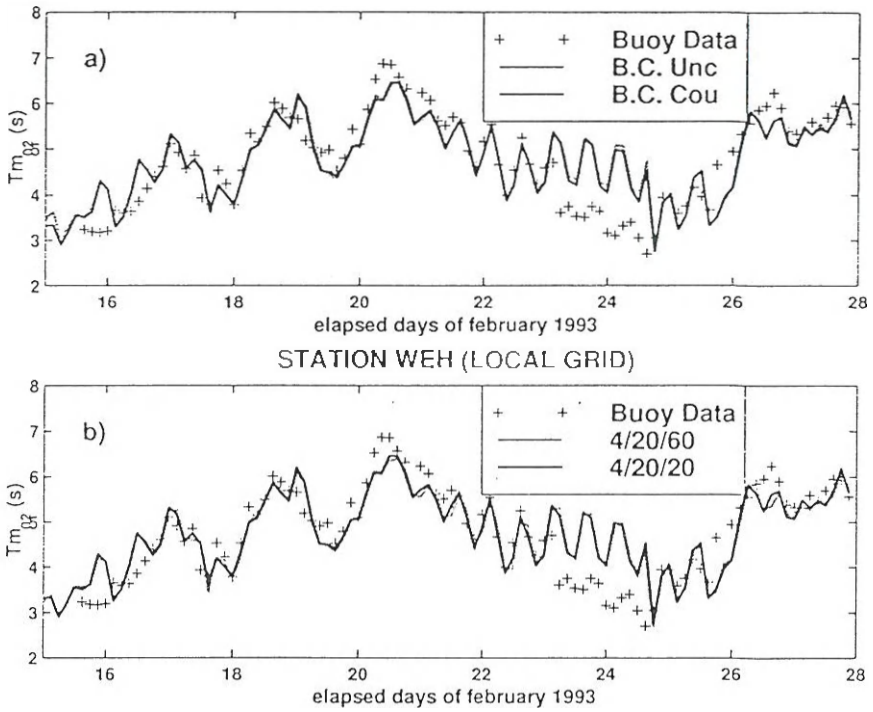

Figure 5: Time series showing the sensitivity to: (a) boundary conditions, and (b) information exchange of Tm_{02} at station WEH.

4.4 Sensitivity to frequency of information exchange

In a coupled system, an important factor to define is the frequency of information transfer between model components. In this work, hydrodynamic fields were updated every 20 minutes (standard coupled mode), which seems suitable for the temporal scale of tide variability. In order to investigate the sensitivity of the model results to the frequency of information exchange, the coupled model on the local grid was also run with an update of the hydrodynamic fields every 60min. The results were compared with those of the standard run. The time series of Tm_{02} presented in Figure 5b, show differences smaller than 5%. Some details in the modulation are missed. For this spatial scale and with current and depth fields which vary only slowly in time and space, the main variation in the spectral periods are well reproduced by the Doppler shift. As one can observe from the time series, the tidal modulations respond mainly to the semidiurnal tidal constituent M2. Further decrease of the frequency of information exchange will lead to increased loss of information.

have a linear 'Phillips' term in its wind input source function. It was not investigated in how far this is responsible for the lack of growth in the uncoupled version.

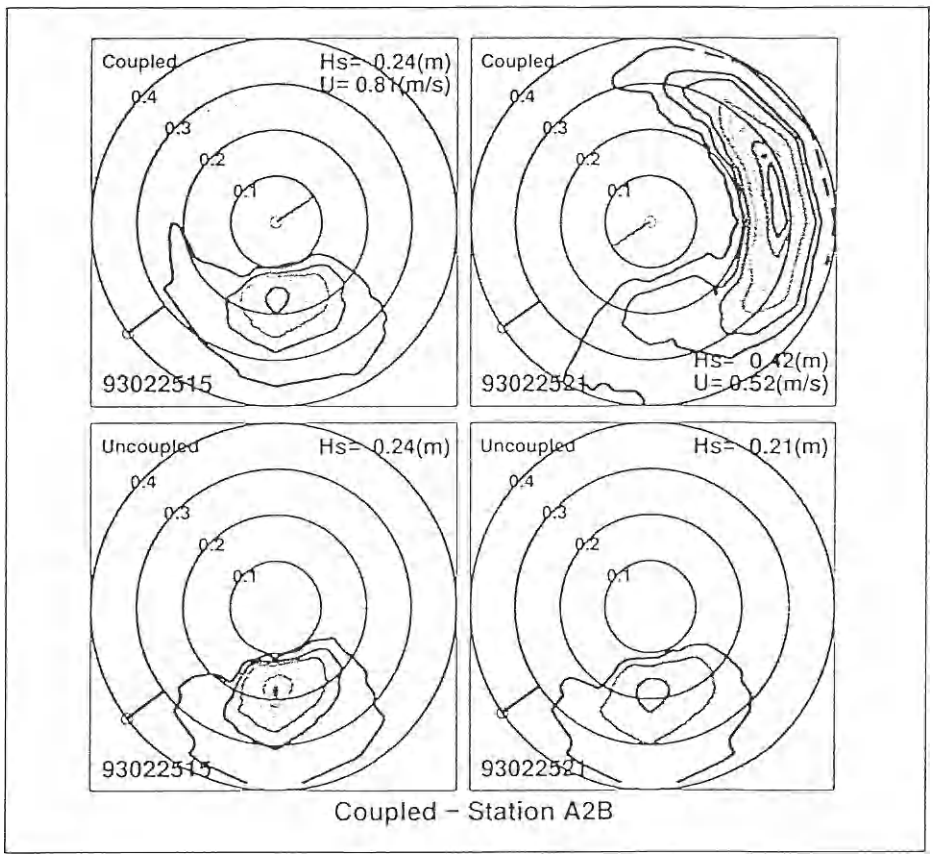

Figure 7: 2D spectra at station A2B calculated by WAM coupled and uncoupled. Significant wave height (Hs), wind direction (dark line) and date are always indicated. For coupled results, current magnitude (U) and current direction (light line) are indicated. The same contour labels were used in all figures (1, 5, and from 10 to 100% every 10% of $0.1 m^2/Hz/deg$).

4.6 Further work

The fine grid bathymetry for the Flemish Coast is much more complicated than can be anticipated from Figure 2. Many sand banks more or less parallel with the coast are present. Their spatial scale is small such that they dissapear from the local grid resolution. A fine grid wave model was nested in the local grid (see section 3.1). For the hydrodynamic fields linear interpolation from the CSM-grid (equal to the local wave model grid) to the fine grid was used. Comparison of time series at A2B from the local and fine grids showed only negligible differences. This is not unexpected since all the variability in the current field induced by the local bathymetry is not represented in the interpolated current field. If the details of the bathymetry are not taken into account in the calculation of the hydrodynamical variables, the directions of the waves and the currents become more and more perpendicular as

Hubbert, K.P., and J. Wolf, 1991: Numerical investigation of depth and current refraction of waves. *J. Geophys. Res.*, 96, 2737–2748.

Holthuijsen, L., and H.L. Tolman, 1991: Effects of the Gulf Stream on ocean waves. *J. Geophys. Res.*, 96, 12755–12771.

Jonsson, I.G, 1990: Wave-current interactions. In B. Le Mehaute and D.M. Hanes (Eds.). *The Sea*, Ocean Engineering Science, Vol 9(A), p65–120. Wiley, New York.

Komen, G.J., L. Cavaleri, M. Donelan, K. Hasselmann, S. Hasselmann, and P.A.E.M. Janssen, 1994: *Dynamics and modelling of ocean waves.* Cambridge University Press.

Luo, W., and J. Monbaliu, 1994: Effects of the bottom friction formulation on the energy balance for gravity waves in shallow water. *J. Geophys. Res.*, 99, 18501–18511.

Luo, W., J. Monbaliu, and J. Berlamont, 1996: Bottom friction dissipation in the Belgian coastal region. *Proc. 25th Int. Conf. Coastal Eng.*, Florida, 836–849.

Luo, W., and M. Sclavo, 1997: Improvement of the third generation WAM model (Cycle 4) for applications in nearshore regions. Internal report no. 116, Proudman Oceanographic Laboratory.

Monbaliu, J., R. Padilla, P. Osuna, R. Flather, J. Hargreaves, J.C. Carretero, S. Espinar, and H. Günther, 1998: A shallow water version of the WAM spectral wave model. Report nr. 52, Proudman Oceanographic Laboratory. *To be published.*

Mastenbroek, C., G. Burgers, and P.A.E.M. Janssen, 1993: The dynamical coupling of a wave model and a storm surge model through the atmospheric boundary layer. *J. Phys. Oceanogr.*, 23, 1856–1866.

Mei, C.C., S. Fan, and K. Jin, 1997: Resuspension and transport of fine sediments by waves. *J. Geophys. Res.*, 102, 15807–15821.

Shemdin, O.H., S.V. Hsiao, H.E. Carlson, K. Hasselmann, and K. Schulze, 1980: Mechanisms of wave transformation in finite-depth water. *J. Geophys. Res.* 85, 5012-5018.

Tolman, H.L., 1990: Wind wave propagation in tidal seas. *Communications on hydraulic and geotechnical engineering*, Delft University of Technology. Report nr. 90–1.

Washington, W.M., and C.L. Parkinson, 1986: *An introduntion to three-dimensional climate modelling.* Oxford University Press.

Yu, C.S., 1993: Modelling Shelf Sea Dynamics, Ph.D. thesis, Department of Civil Engineering, K.U.Leuven, Belgium.